Arabian Journal for Science and Engineering (2023) 48:9383–9399
https://doi.org/10.1007/s13369-022-07503-z

RESEARCH ARTICLE-PETROLEUM ENGINEERING

Inhibition of Barium Sulfate Precipitation During Water Injection into Oil Reservoirs Using Various Scale Inhibitors

Azizollah Khormali[1] · **Soroush Ahmadi**[2] · **Yousef Kazemzadeh**[3]

Received: 13 October 2021 / Accepted: 17 November 2022 / Published online: 28 November 2022

Abstract
In this work, barium sulfate precipitation was analyzed under ambient and reservoir conditions. The worst scenario for barium sulfate precipitation occurred at a mixing ratio of 40:60 formation and injection waters. This ratio was used in the jar, turbidity, dynamic tube blocking, and coreflood tests. In addition, a critical radius and mass of barite particles were determined at various values of supersaturation ratio and surface tension. For the prevention of barium sulfate precipitation, three well-known industrial scale inhibitors and one recently developed reagent (named DPAAI) were used. Results of static and dynamic tests indicated that DPAAI had the best performance for inhibiting barium sulfate precipitation. Moreover, DPAAI could prevent the heterogeneous nucleation of barium sulfate and was effective in blocking the formation of barite and inhibiting crystal growth. The chances of collisions between the cations and anions in the solution were significantly reduced in the presence of DPAAI. The rock permeability due to barium sulfate was reduced to less than 40% of the initial permeability. After the application of the inhibitors, the formation damage was considerably reduced. Besides, a correlation has been developed to predict the reduction in rock permeability owing to the precipitation of barium sulfate in rock samples. Meanwhile, it was found that data predicted by the model were in good agreement with experimental data. Furthermore, scale inhibitor return concentration was evaluated by modeling and experiments, on the basis of which the protection period of the near-wellbore region and well from barium sulfate was determined. Among the investigated reagents, the longest squeeze lifetime was observed for DPAAI, which was associated with the intensification of adsorption and desorption processes on the rock surface.

Keywords Barium sulfate · Formation damage · Scale inhibitor · Squeeze lifetime · Simulation

1 Introduction

Currently, scaling is one of the main complications manifested during production operation in oilfields. Prediction of inorganic salts reduces the mean time between failures of the equipment and causes formation damage. In particular, the precipitation of salts on the electrical submersible pumps (ESPs) disrupts heat transfer and leads to jamming of the electric motor, shaft breakage, and pump failure [1–5]. The reason for the salt precipitation is the supersaturation of a solution with ions [6–9]. BinMerdhah [10] reported that the precipitation of barium sulfate is decreased by increasing temperature, as its solubility is increased. It should be noted that during the operation of ESP, the fluid is heated when it passes through the submersible electric motor and the pump itself, and consequently, due to the increased solubility of barium sulfate upon heating, salt precipitation on the ESP impellers may be reduced. However, this is not observed in practice. Thus, the main reason for the precipitation of barium sulfate is the mixing of incompatible formation and injection waters during waterflooding [11–14]. In this regard, the near-wellbore region and equipment operating under the conditions of water injection are exposed to the precipitation of sulfate scales. Besides, in the process of raising the production fluid from the bottomhole to the wellhead, the chemical

✉ Azizollah Khormali
aziz.khormaly.put@gmail.com; a.khormali@gonbad.ac.ir

1 Department of Chemistry, Faculty of Basic Sciences and Engineering, Gonbad Kavous University, Gonbad Kavous, Iran

2 Department of Chemical Engineering, Faculty of Engineering,, Payame Noor University, PO Box 19395-4697, Tehran, Iran

3 Department of Petroleum Engineering, Faculty of Petroleum, Gas, and Petrochemical Engineering, Persian Gulf University, Bushehr, Iran

equilibrium is disturbed due to the change in temperature and pressure. This is accompanied by the precipitation of inorganic salts on the walls of the tubing and impellers of the pumps, which reduces the oil production rate [15, 16].

When the spontaneous formation of solid particles in a solution occurs, the total energy of the system is decreased. Moreover, the formation of salt crystals in the solutions is completed in metastable systems, whose states are often quite significantly different from the equilibrium ones. The growth of formed crystals occurs due to a decrease in their free surface energy. This energy is rapidly decreased with an increase in the radius of the particles after reaching the critical size [6, 17–19]. This means that the large crystals will continue to grow, and the small crystals can dissolve again. Moreover, organic particles having high adhesive properties can serve as nuclei of scale formation by adhering to the surface equipment. Therefore, the formation and growth of salt deposits on the surface of the production equipment can be intensified in the presence of natural organic active components of oil [20, 21]. This effect can be considered in the following steps: I) Chemical process—under the action of active organic components of oil, the phase equilibrium is disturbed, resulting in the formation of insoluble salts. II) Physicochemical process—the active organic components of the oil are involved in the adsorption processes and provide adhesion both to each other and to the equipment surface and, ultimately, cause the crystal growth [13, 20, 22].

The properties of the barium sulfate precipitates depend on the ratio of the following rates: crystal nucleation rate and growth rate. When two types of water are mixed, the solution can be characterized by the concentration of barium sulfate that can be either less than the solubility limit or more at a given mineralization, pressure, and temperature [23–25]. It is obvious that crystal nuclei cannot form and grow in the first case. Furthermore, to predict the place of barium sulfate precipitation, it is necessary to study the kinetics of the formation of barium sulfate during mixing water with different concentrations of sulfate and barium ions. To describe the kinetics, the curves of the change in the optical density over time at various concentrations of barium and sulfate ions are utilized [21, 26, 27].

The control of salt precipitation in the downhole equipment and near-wellbore region does not have a universal approach. Scale inhibitors are widely used to prevent the deposition of inorganic salts. An effective reagent should inhibit scaling over a long period. The protection period of the production equipment and near-wellbore region from the salt precipitation mainly depends on the chemical composition, pressure, temperature and pH, adsorption capacity of the reservoir rock, and type of the scale inhibitor [28–32]. In special cases, such as formations with high adsorption capacity and low water production rates, the protection period with the use of scale inhibitors can be significantly increased. To increase the scale inhibition, several types of additives can be used in the inhibitor packages and reagents with different mechanisms can be injected into the reservoir. It is no coincidence that many scale inhibitors produced recently have complex compositions [33–37]. Thus, one of the promising directions for controlling scale formation is the application of the mixture of reagents. The mechanisms of action of the scale inhibitors are based on blocking the crystallization centers, suppressing the growth of salt crystals, and keeping them in a suspended state [38–43].

Different scale inhibitors are developed to prevent inorganic salt precipitation in the petroleum industry. Mady et al. [44] synthesized and investigated phosphonated polyetheramine scale inhibitors for calcite and barite control in oil wells. They evaluated the inhibition performance of the reagents by performing static and dynamic tests. They concluded that the mixture is more effective than commercial scale inhibitors of DTPMP (diethylenetriamine penta) and ATMP (aminotrimethylene phosphonic acid) under laboratory conditions. In addition, the turbidity tests confirmed the results of static and dynamic tests. Kommanapalli et al. [45] used a new copolymer of maleic acid-sodium methallyl disulfonate for preventing barium sulfate. They mentioned that the crystallization processes of barium sulfate are complicated due to its low solubility over a wide range of pressures and temperatures. The inhibition mechanism of the used reagent was based on the reduction in the crystal growth rate. They observed that the scale inhibitor has the highest efficiency for the prevention of barium sulfate precipitation at an optimal concentration. BinMerdhah [10] studied the prevention of barium sulfate precipitation by the static jar and coreflood tests using DTPMP and polyphosphino carboxylic acid (PPCA). The author reported that the maximum precipitation of barium sulfate occurred at a certain ratio of water, which should be used in the evaluation of the scale inhibition performance. In the coreflood tests, the used inhibitors could prevent $BaSO_4$ formation in the porous media and considerably reduce the formation damage.

In this work, it is aimed to predict barium sulfate precipitation under ambient and reservoir conditions. For this purpose, scaling tendency, saturation index, and salt concentration are investigated. Also, the critical radius and mass of barium sulfate salts in the absence of scale inhibitors are examined. The effectiveness of a novel and three well-known industrial scale inhibitors is studied to prevent barium sulfate precipitation under various conditions. To determine the optimal concentration of the reagents, the scale inhibition efficiency is analyzed through the jar tests under different conditions. The results obtained in the jar tests are also confirmed by measuring the turbidity values. Moreover, to analyze the performance of the scale inhibitors, the critical supersaturation ratio is evaluated. Furthermore, the influence of $BaSO_4$ precipitation on rock permeability is assessed by conducting

coreflood tests in the presence and absence of the reagents. Besides, a new model is developed for predicting formation damage using experimental data on changes in rock permeability. As a final step, the return scale inhibitor concentration will be determined through modeling and experimental analysis. The novelty of this work is the first application of the newly developed mixture (DPAAI) for barium sulfate inhibition by various experiments, which has a higher inhibition performance in comparison with the industrial reagents and a longer squeeze lifetime. In our previous work, this mixture was evaluated only for the inhibition of calcium and strontium sulfate scales. In contrast to industrial inhibitors, no corrosive effect is observed in the presence of DPAAI. In addition, a new model was developed for the prediction of rock permeability reduction due to barite precipitation, which had high accuracy, and the predicted data by the model were in good agreement with experimental data.

2 Materials and Methods

All conducted experiments are based on international standards and completely cover the engineering aspects of scale control using inhibitors before field application.

2.1 Ion Content of the Brines

Formation (FW) and injection (IW) waters with different ion concentrations were used to assess the possibility of barium sulfate precipitation and to study the inhibitory ability of chemical reagents under various conditions. The ion concentrations of the used brines are shown in Table 1. As shown in this table, FW and IW consist of barium and sulfate ions. A mixture of FW and IW can be prone to the precipitation of barium sulfate salt.

In this work, the prediction of barium sulfate precipitation in a mixture of the brines was carried out using the OLI ScaleChem program. For this purpose, the concentration of the ions in FW and IW was utilized. In the program, the input data were as follows: pressure, temperature, ion content of waters, and mixing ratio. Scaling tendency (ST) and amount of salt precipitation were the output data on the scaling prediction. In addition, saturation index (SI) of barium sulfate was determined using ST values. SI is defined as the logarithm of ST [46]. ST, SI, and salt precipitation of barium sulfate were investigated under ambient ($P = 1$ atm, $T = 25$ °C) and reservoir ($P = 247$ atm, T = 75 °C) conditions.

Table 1 Ion concentration of the used synthetic waters

Ion	Ion concentration (ppm)	
	Synthetic formation water (FW)	Synthetic injection water (IW)
Sodium	33,582	12,035
Potassium	1427	368
Magnesium	1258	1466
Barium	195	0
Chloride	72,914	19,854
Sulfate	218	2934
TDS	109,594	36,657

2.2 Critical Radius and Mass of Barium Sulfate Particles

Precipitation of a salt particle occurs when its size and mass exceed a critical value [6]. The critical radius for barium sulfate particles was determined using the Kelvin equation as follows:

$$r_c = \frac{500 \times \sigma \mathrm{MW}}{\rho_s R(T + 273)\ln(\mathrm{SSR})} \tag{1}$$

$$m_c = \rho_s \times \frac{4\pi r_c^3}{3} \tag{2}$$

where r_c is the critical radius, m; σ is the surface tension on the boundary of the solid particle and solution, N/m; MW is the molecular weight, gr/mol; ρ_s is the average density of barium sulfate salts, Kg/m^3; R is the molar gas constant, 8.314 J/(mol. K); T is the temperature, °C; SSR is the supersaturation ratio; m_c is the critical mass, kg. In this study, the effect of the supersaturation ratio on the critical radius and mass was studied at two different values of surface tension without the use of the reagents.

2.3 Evaluation of the Scale Inhibitors by Jar and Turbidity Tests

A new (DPAAI) [8] and three well-known industrial and scale inhibitors were used to prevent barium sulfate precipitation under a variety of conditions. The inhibitors used in this work are shown in Table 2. The used reagents are effective in blocking the formation of barite and inhibiting crystal growth. It should be noted the scan images of the barite particles in the presence of scale inhibitors can provide helpful information about the reduction in crystal growth rate, which is a topic for future work. Experimental studies on the evaluation of the performance of the scale inhibitors under static conditions were completed by conducting jar and turbidity tests. The detail of each test is presented below.

Table 2 The used scale inhibitors

Scale inhibitor number	Abbreviation	Name and composition
1	HMDP	hexamethylenediamine tetramethylene phosphonic acid
2	DTPMP	diethylenetriamine penta
3	PBTC	2-phosphonobutane-1,2,4-tricarboxylic acid
4	DPAAI [8]	DTPMP (12%), PBTC (6%), ATMP—aminotrimethylene phosphonic acid (12%), NH_4HF_2 (3%), C_3H_8O alcohol (2%), H_2O (65%)

2.3.1 Jar Test

Jar tests were completed to analyze the inhibition efficiency of the reagents and determine their optimal concentration in preventing barium sulfate precipitation. The tests were carried out by measuring Ba^{2+} concentration with and without inhibitors. The working solution for each test was prepared using FW and IW at a ratio of 40:60. At this mixing ratio, the worst scenario of barium sulfate precipitation occurred (it was explained in Sect. 3.1). When the barium sulfate is precipitated, the concentration of the barium ions in the working solution is reduced [14]. The jar tests were carried out at 75 °C. The time of each test was 48 h, which was sufficient to assess the scale inhibition performance. The barium ion concentration was measured using an ion meter. In the jar tests, the reagents were utilized in a range from 5 to 35 ppm in order to determine the optimal concentration. Three barium ion concentrations were measured during the tests as follows: (1) $[Ba^{2+}]_0$: initial concentration of the barium ions before testing; (2) $[Ba^{2+}]_1$: concentration of barium ions after testing with reagents; (3) $[Ba^{2+}]_2$: concentration of barium ions after testing without reagents (a blank case). The jar tests were performed in accordance with the standard NACE TM0374-2016. The inhibition efficiency (IE) of the inhibitors has been determined as follows:

$$\mathrm{IE} = \frac{[\mathrm{Ba}^{2+}]_2 - [\mathrm{Ba}^{2+}]_1}{[\mathrm{Ba}^{2+}]_2 - [\mathrm{Ba}^{2+}]_0} \times 100 \tag{3}$$

To analyze the influence of barium ion concentration on the inhibition efficiency of the reagents, the jar tests were performed at various concentrations of barium ions. For this purpose, Ba^{2+} concentration in FW was changed from 200 to 2000 ppm. The scale inhibitors were utilized at 20 ppm, which was the optimal concentration under static conditions (based on the results obtained in Sect. 3.3, Fig. 4a). It should be noted that other conditions such as temperature (75 °C), test duration (48 h), and mixing ratio (40:60 for FW: IW) remained unchanged.

2.3.2 Turbidity Test

The turbidity test is a well-known experiment to evaluate the inhibition performance of the reagents under static conditions. In modern analytical practice, the turbidity value is a fairly important indicator for studying salt precipitation in an aqueous solution [47]. In this test, a solution of FW and IW at a ratio of 40:60 was used. The turbidity tests were performed using a turbidimeter with and without reagents. The reagents were utilized at concentrations of 10 and 20 ppm to verify the optimal concentrations obtained in the jar tests. The light scattering by suspended solid particles of the working solution was measured. For this purpose, the solution was illuminated with a stream of light with an intensity of I_0, and then, the intensity of the transmitted radiation (I_1) was measured. When the light passes through the solution, the smallest particles absorb and scatter part of the light. As a result, the output light intensity was reduced. If an inhibitor can efficiently prevent salt precipitation, there will be more particles in the suspension, and hence, the intensity of the transmitted light will be less [4]. Therefore, a high inhibition performance is observed at low values of turbidity.

2.4 Dynamic Tube Blocking Test

These tests have been completed to determine the minimum inhibitory concentration (MIC) of the reagents during $BaSO_4$ prevention under dynamic conditions. Toward this end, a coreflood apparatus was utilized (as illustrated in Fig. 1). In this case, the formation and injection waters were pumped into a coil (tube) with a radius and length of 0.0005 m and 1 m at a mixing ratio of 40:60 FW: IW. The mixing ratio was adjusted through the injection rate. The tests were performed by measuring the pressure drop across the coil at 75 °C. The inhibitor concentration was increased in steps from 0 ppm (a blank case) to 30 ppm. The reagents were added to the tank containing IW. The test duration was 120 min.

2.5 Coreflood Tests

Coreflood experiments have been conducted to assess the formation damage owing to $BaSO_4$ precipitation and to

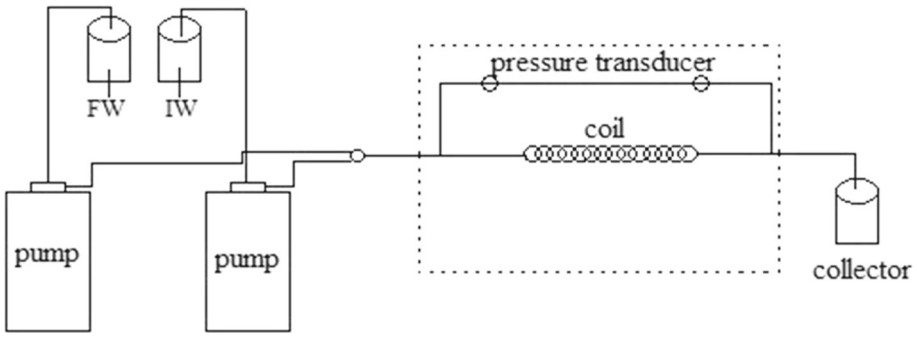

Fig. 1 The used apparatus in coil blocking experiments

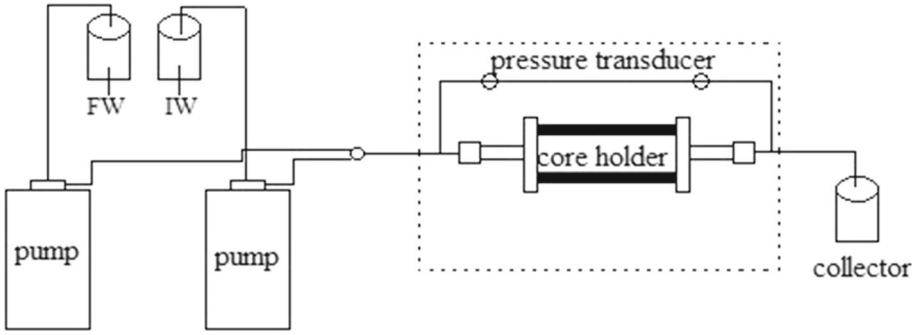

Fig. 2 The used coreflood apparatus

determine the inhibitor concentration profile (adsorption and desorption processes). For this purpose, a coreflood apparatus, the schematic diagram of which is presented in Fig. 2, was used. In the apparatus, the formation and injection waters were mixed at a ratio of 40:60. The ratio was applied by adjusting the injection rate in the pumps. The initial porosity and permeability of the core samples used in the tests were 0.18 and 27 mD. In addition, the diameter and length of the samples were 3.5 cm and 6 cm. The main lithology of the core samples was limestone and dolomite.

2.5.1 Formation Damage Evaluation

To analyze the formation damage caused by $BaSO_4$, the working solution (40:60 FW:IW) was pumped into the carbonate rocks with a constant injection rate in each pump. The tests have been performed at 75 °C. In this case, the rock permeability was evaluated in a range of pore volume injected (PV_{inj}) from 0 to 35. The rock permeability was determined by the linear Darcy formula [48]:

$$K = \frac{16.67 \times q\mu L}{A\Delta P} \tag{4}$$

where K is the rock permeability (mD); q is the rate of injection into the rock samples (mL/min); μ is viscosity (cP); L is the length of the samples (cm); A is cross-sectional area (cm^2); ΔP is pressure drop across core samples measured by a pressure transducer (Pa).

The formation damage assessment was carried out with and without reagents. The inhibitors were added to the injection water at MIC, which was determined in dynamic tube blocking tests. DPAAI and DTPMP at 20 ppm, PBTC, and HMDP at 25 ppm were used (MIC of the inhibitors has been explained in detail in Sect. 3.5). In this case, the graph of rock permeability ratio (K_f/K_i) was plotted for 35 PV_{inj}. K_f is the damaged rock permeability during the solution injection into the samples. PV_{inj} was determined by the following equation [46]:

$$PV_{inj} = \frac{qt}{\pi r^2 L\phi} \tag{5}$$

where PV_{inj} is the pore volume injected (unitless); t is the injection time (s); r is the radius of rock samples (cm); ϕ is the initial porosity of rock samples (unitless).

2.5.2 Scale Inhibitor Return Concentration

To study the adsorption–desorption processes of used inhibitors during the prevention of $BaSO_4$ precipitation, a series of coreflood experiments were carried out. For this purpose, the scale inhibitors at MIC were added to the injection water. At the same time, the concentration of the scale inhibitors at the outlet of the core holder was analyzed over time. The injection of scale inhibitors into the core samples was stopped when the inlet and outlet concentrations were equal. Core samples containing inhibitors were kept for 2 h for complete adsorption of the reagents.

Table 3 Experimental uncertainties

Parameter	Max uncertainties
Inhibition efficiency	± 0.5%
Temperature	± 0.2 °C
Inhibitor concentration	± 0.4 ppm
Pressure drop	± 1 Pa
Light transmittance ratio	± 2%
Surface tension	± 0.5 mN/m
Permeability ratio	± 0.5%
Injection rate	± 0.1 mL/min
Inhibitor concentration ratio in coreflood	± 0.2%

Thereafter, the return concentration of the reagents was investigated for 35 PV_{inj} in order to evaluate the desorption process. For this purpose, only formation water was injected. IW and scale inhibitors were not pumped. In this case, scale inhibitor concentration at the outlet was determined by measuring the concentration of phosphate ions. The photometric method was used to measure the concentration of scale inhibitors during the desorption process. This method is based on the reaction of phosphate ions with molybdate ions in an acidic medium.

2.6 Uncertainty Analysis

The confidence intervals (CI) of the measured parameters were determined as follows:

$$\mathrm{CI} = \bar{\mathrm{x}} \pm z\frac{S}{n} \tag{6}$$

where $\bar{\mathrm{x}}$ is the arithmetic average of the observed data; s is the standard deviation (error); z is the value of the desired confidence level; n is the number of tests. An analysis of the uncertainty of the measured parameters was carried out, the results of which are presented in Table 3.

3 Results and Discussion

3.1 Prediction of Barium Sulfate Precipitation

Scaling tendency and precipitation of barium sulfate were determined using the OLI ScaleChem program under ambient (P = 1 atm, T = 25 °C) and reservoir (P = 247 atm, T = 75 °C) conditions. The results are shown in Table 4. As presented in the table, scaling tendency, saturation index, and precipitation of barium sulfate were significantly influenced by the mixing ratio of FW and IW. The worst scenario for the barium sulfate precipitation in both cases was observed at 40:60 FW: IW. Accordingly, the ratio of 40:60 FW: IW will be used in the next experiments to study the inhibition efficiency in preventing barium sulfate formation under a variety of conditions. Moreover, Table 4 depicts the influence of P and T on barium sulfate scale formation. The salt concentration (precipitation) was decreased by increasing pressure and temperature. This behavior is associated with an increase in $BaSO_4$ solubility due to the increase in P and T.

In addition, the amount of salt precipitation was measured by running experiments at various mixing ratios of synthetic waters to confirm that the worst-case scenario for barium sulfate formation occurs at 40:60 FW: IW. The tests were completed at room conditions by measuring the amount of salt precipitated per volume of solution. The obtained results

Table 4 Prediction of barium sulfate precipitation under ambient and reservoir conditions

FW%	Ambient conditions: P = 1 atm (0.1013 MPa), T = 25 °C			FW %	Reservoir conditions: P = 247 atm (25.0272 MPa), T = 75 °C		
	Scaling tendency	Saturation index	Salt precipitation (ppm)		Scaling tendency	Saturation index	Salt precipitation (ppm)
100	35.6	1.6	14.9	100	22.8	1.4	13.2
90	48.1	1.7	25.7	90	39.4	1.6	22.7
80	65.7	1.8	44.5	80	55.7	1.7	39.7
70	98.4	2.0	62.6	70	72.8	1.9	55.9
60	129.6	2.1	89.1	60	95.7	2.0	69.4
50	155.2	2.2	102.7	50	111.2	2.0	90.1
40	*195.5*	*2.3*	*124.6*	*40*	*125.6*	*2.1*	*99.4*
30	162.7	2.2	90.5	30	85.7	1.9	76.4
20	102.3	2.0	59.8	20	49.6	1.7	49.2
10	55.4	1.7	26.4	10	26.4	1.4	19.5
0	0	–	0	0	0	–	0

Table 5 The laboratory results of the measurement of barium sulfate precipitation under room conditions at different mixing ratios

FW %	Salt precipitation (ppm)
90	26.1
80	46.2
70	61.2
60	90.9
50	105.2
40	*128.4*
30	88.4
20	62.4
10	24.7

are presented in Table 5. As can be seen from the table, the maximum amount of precipitated salts occurred at a mixing ratio of 40:60 FW: IW. Consequently, further tests are carried out at this mixture ratio.

3.2 Results of Determination of the Critical Radius and Mass of Barium Sulfate Salts

Barium sulfate precipitation, its critical mass and radius were estimated at two different values of surface tension on the boundary of salt particles and solution using Eqs. 1 and 2. This test was completed without the use of scale inhibitors. As illustrated in Fig. 3, the critical radius and, accordingly, the critical mass was decreased by increasing the supersaturation ratio with barium sulfate. Salt crystallization occurs when the amount of formed salt exceeds the critical mass [49]. In addition, the critical radius and mass were increased by increasing the surface tension. Moreover, a critical supersaturation ratio with barium sulfate salts was observed when the critical mass has reached a minimum constant value. For the surface tensions of 58 and 113 mN/m, the critical supersaturation ratio with barium sulfate was 3 and 4, respectively. It should be taken into account that the precipitation of particles occurs when the supersaturation ratio with the salt exceeds the critical value [50]. Figure 3 illustrates that the critical mass and radius of solid particles were considerably reduced until the supersaturation ratio has reached the critical value. This behavior is due to the fact that the solubility of $BaSO_4$ is significantly decreased when the concentration and supersaturation ratio exceeds the critical value.

3.3 Results of the Jar and Turbidity Tests in Preventing $BaSO_4$ Precipitation

Figure 4 illustrates the results of jar tests on the evaluation of inhibition performance of the reagents in preventing barium sulfate precipitation under static conditions. The tests were varied out at 75 °C. Figure 4a depicts the efficiency at various concentrations of the inhibitors at a ratio of 40:60 FW:IW. The efficiency of reagents was increased with an increase in the concentration, which is associated with strengthening the mechanism of the reagents in barium sulfate prevention. As depicted in Fig. 4a, the optimal concentrations of scale inhibitors were about 20 ppm (for DPAAI, DTPMP) and 25 ppm (for PBTC, HMDP). At concentrations higher than the optimal values, the inhibition efficiency remained unchanged with a further increase in the concentration. Among the examined inhibitors, DPAAI had the best performance for inhibiting barium sulfate precipitation. The efficiency of DPAAI, DTPMP, PBTC, and HMPD at optimal concentrations was 95.7, 88.5, 87.5, and 85.9%, respectively. DPAAI as a multicomponent scale inhibitor showed a positive synergistic inhibition effect and which prevented the heterogeneous nucleation of barium sulfate particles. In addition, the collision probability between cations and anions in the solution with the use of DPAAI was reduced. DPAAI could specifically adsorb the barium sulfate crystals, slow down the crystal growth rate, and keep them in suspension in the solution. Furthermore, Fig. 4b shows the effect of Ba^{2+} concentration on the inhibition performance of reagents at 20 ppm. In the tests, the concentration of barium ions in the formation water was increased to 2000 ppm, and the waters were mixed at a ratio of 40:60 at 75 °C. As presented in the figure, the average reduction in the inhibition efficiency of all reagents was about 3.5% compared to the concentration of 195 ppm for barium ions. Here, DPAAI was the most effective reagent for inhibiting barium sulfate precipitation. The scale inhibition efficiency of DPAAI was more than 92.8% at any studied concentration of barium ions. The high inhibition performance of the reagents is related to the strong interaction of $PO_2{}^{-3}$ groups in their structure with the crystal of barium sulfate scales and the subsequent effect on the crystal morphology, which ultimately reduces its growth rate [51]. More detailed information on the inhibition mechanism of the used reagents in the prevention of scale formation is presented in our previous work [8].

Figure 5 depicts the results of turbidity tests at concentrations of 10 and 20 ppm of the scale inhibitors. The tests were conducted under ambient conditions, as the worst scenario of barium sulfate precipitation occurred in low pressure–temperature conditions. As presented in the figure, the turbidity values were significantly decreased after adding reagents to the solution compared to the blank case. This behavior is related to the inhibition of $BaSO_4$ by reagents, as a consequence of which the solid particles are suspended and the light intensity is reduced. At the same time, Fig. 5 depicts that the decrease in turbidity values at 20 ppm of the reagents was greater than at 10 ppm. At both concentrations, the lowest values of turbidity values were observed in the presence of DPAAI. Therefore, turbidity analysis confirms that DPAAI

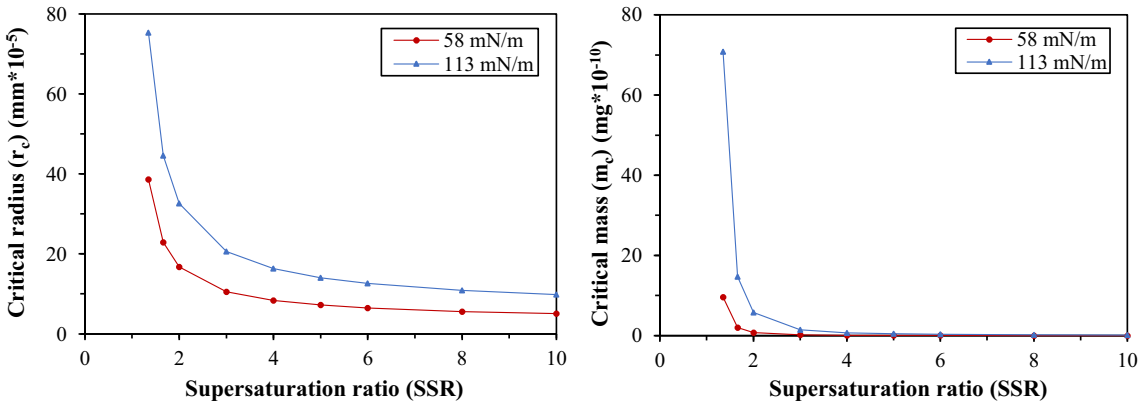

Fig. 3 Dependence of the critical radius and critical mass of barium sulfate particles on the supersaturation ratio

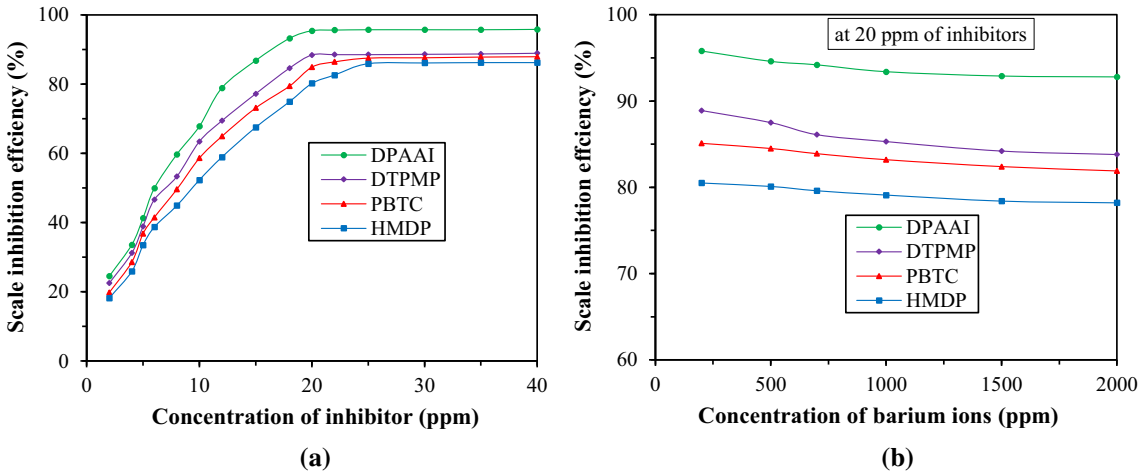

Fig. 4 Scale inhibition efficiency at various concentrations of the reagents at a mixing ratio of 40:60 FW: IW **a**, and at different concentrations of barium ions in the solution at 20 ppm of the reagents **b**

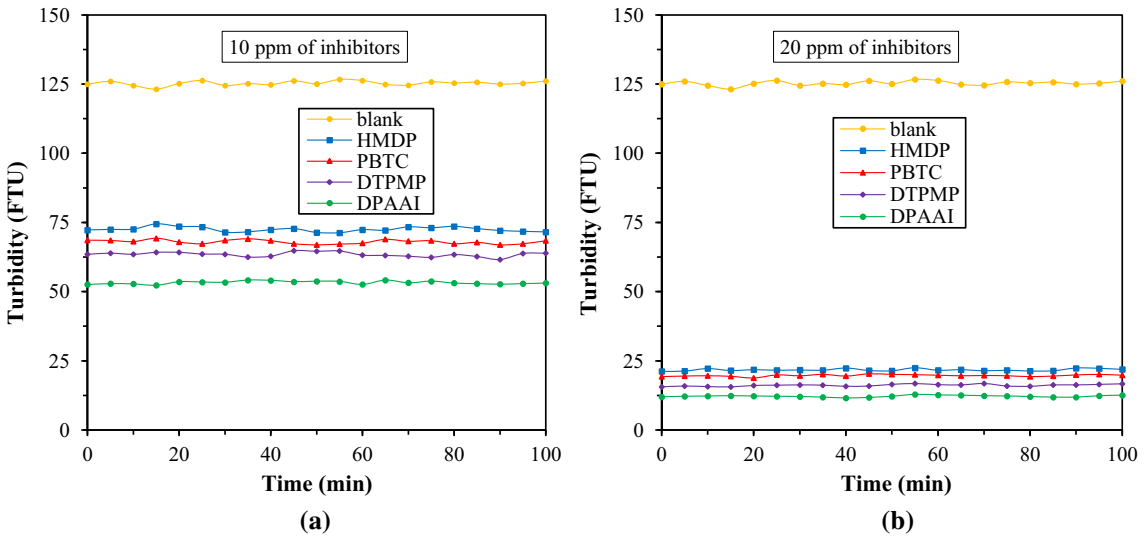

Fig. 5 Changes in the turbidity values of the solution with and without the use of inhibitors at 10 ppm **a**, and 20 ppm **b**

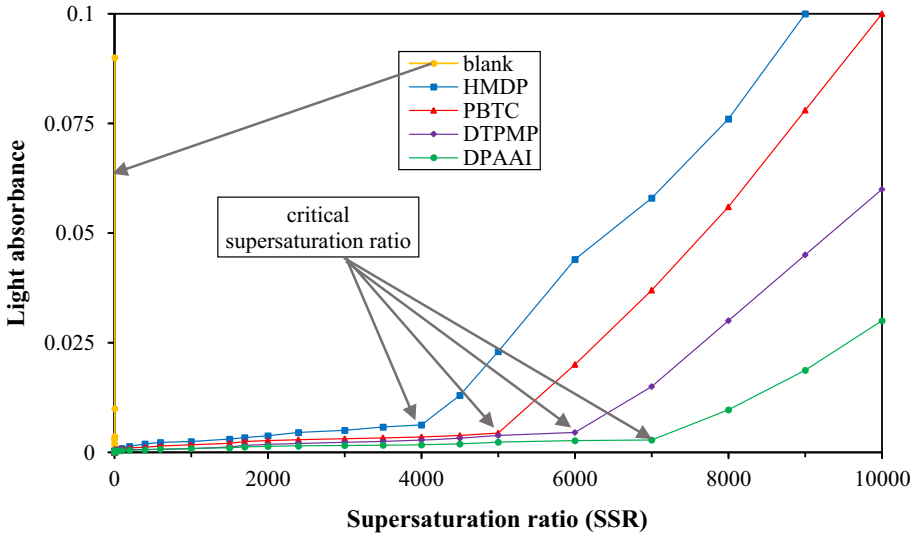

Fig. 6 Dependence of light absorbance on the supersaturation ratio with barium sulfate salts

has the highest inhibition efficiency in preventing barium sulfate precipitation under static conditions. The high inhibition performance of DPAAI is related to its ability to inhibit salt precipitation and provide more particles in suspension.

3.4 Results of Study on Critical Supersaturation Ratio

Figure 6 illustrates the results of light absorbance through the solution depending on the supersaturation ratio with barium sulfate. The purpose of this experiment is to assess the critical supersaturation ratio with the barium sulfate salts using scale inhibitors. When the value of the supersaturation ratio is above the critical value, the salt is precipitated, and therefore, the scale inhibitor cannot effectively prevent scale formation. It should be noted that the critical supersaturation ratio without the use of scale inhibitors at surface tensions of 58 and 113 mN/m was 3 and 4, respectively (Sect. 3.2). As shown in Fig. 6, the light absorbance was significantly increased when the supersaturation ratio was above the critical ratio. As presented in this figure, with the use of HMDP, PBTC, DTPMP, and DPAAI, the critical supersaturation ratio was 4000, 5000, 6000, and 7000, respectively. The higher value of the critical supersaturation ratio in the presence of DPAAI is explained by its higher inhibition efficiency for preventing barium sulfate precipitation under static conditions. It should be noted the studied scale inhibitors are effective crystal growth reagents in controlling the crystallization rate of barite [51]. Thus, the studied reagents are the crystallization inhibitors that can reduce the deposition rate of barite after the formation of crystals. In the oilfield operation, the supersaturation ratio with the salts exceeding 4000 is not observed [52]. Therefore, the used reagents can inhibit $BaSO_4$ precipitation with high efficiency under reservoir pressure and temperature conditions.

3.5 Results of Coil Blocking Experiments

Dynamic tube blocking experiments were completed to determine MIC for the examined scale inhibitors under dynamic conditions. MIC values will be used in the coreflood experiments. An increase in the pressure drop in the tube caused by barium sulfate precipitation indicates that the used reagent could not prevent salt precipitation at the studied concentration. The results obtained in determining MIC are presented in Table 6. Analysis of the experimental results made it possible to establish the effective concentration of the used scale inhibitors for the application in the coreflood tests. As shown in Table 6, in a blank case (without scale inhibitor), the decrease in pressure was about 250 kPa after 35 min. This behavior is related to the precipitation of barium sulfate in the coil without the use of scale inhibitors that confirm the high potential for salt formation by mixing FW and IW. As presented in Table 6, by increasing the inhibitor concentration, the pressure drop was decreased, indicating the prevention of barium sulfate precipitation at higher concentrations. As can be seen, DPAAI and DTPMP could inhibit salt precipitation under dynamic conditions at 20 ppm. In this case, the pressure drop was not increased during 120 min of solution injection and remained at a low level. Accordingly, DPAAI and DTPMP have a sufficiently high inhibition efficiency at 20 ppm for the control of $BaSO_4$ in dynamic studies. In addition, the MIC of PBTC and HMDP was 25 ppm. These values of MIC will be used in coreflood experiments.

In addition, the pressure drop across the coil tube due to barium sulfate precipitation was evaluated at different injection rates (1, 2, and 3 mL/min) without the use of inhibitors. It was done to determine the influence of the injection rate on the barite formation. The obtained results are presented in Table 7. As can be seen from this table, the pressure drop was decreased by increasing the injection rate. This is due to the

Table 6 Results of pressure changes in dynamic coil blocking tests at an injection rate of 2 mL/min

Concentration (ppm)	Pressure drop, KPa			
	HMDP	DTPMP	PBTC	DPAAI
0	250 (after 35 min)	250 (after 35 min)	250 (after 35 min)	250 (after 35 min)
5	250 (after 48 min)	250 (after 86 min)	250 (after 65 min)	250 (after 120 min)
10	250 (after 116 min)	202 (after 120 min)	246 (after 120 min)	135 (after 120 min)
15	168 (after 120 min)	104 (after 120 min)	142 (after 120 min)	65 (after 120 min)
20	96 (after 120 min)	*19 (after 120 min)*	82 (after 120 min)	*13 (after 120 min)*
25	*23 (after 120 min)*	19 (after 120 min)	*21 (after 120 min)*	12 (after 120 min)
30	23 (after 120 min)	18 (after 120 min)	20 (after 120 min)	11 (after 120 min)

Table 7 Results of pressure drop across the coil tube at different injection rates without the use of inhibitors

Time (min)	Pressure drop (KPa) without the use of inhibitors		
	1 mL/min	2 mL/min	3 mL/min
0	0	0	0
5	12	9	7
10	24	17	14
15	46	33	28
20	67	51	44
25	114	76	62
30	263	122	91
35	–	251	148
40	–	–	259

fact that at high flow rates, the contact time of the injection and formation waters is reduced, so the ions (sulfate and barium) do not have enough time to come together and form the salt. Moreover, dynamic coil tube tests were performed in the presence of DPAAI at injection rates of 1, 2, and 3 mL/min. In this case, the mixture was used at a concentration of 20 ppm. The results showed that the injection rate had no significant effect on the performance of DPAAI. The pressure drop at all studied injection rates with the use of DPAAI was almost the same. Thus, DPAAI is efficient in preventing barite formation under different fluid flow conditions.

3.6 Results of Coreflood Experiments

Coreflood tests have been completed to investigate the changes in the permeability of core samples due to barium sulfate precipitation during waterflooding. In the experiments, FW and IW were mixed and pumped into the rocks at a ratio of 40:60 using the coreflood apparatus under reservoir conditions (75 °C and 25 MPa). Figure 7 illustrates the changes in permeability ratio (K_f/K_i) at various values of pore volume injected. MIC values of the scale inhibitors obtained in the coil blocking experiments were utilized in coreflood tests as follows: DPAAI and DTPMP at 20 ppm; PBTC and HMDP at 25 ppm. As shown in the figure, in the blank case, the rock permeability due to barium sulfate precipitation was reduced to less than 40% of the initial permeability. This decrease in permeability confirms the high tendency of the mixture of formation and injection waters for precipitation of barium sulfate and formation damage. In addition, Fig. 7 depicts that after using the reagents, the permeability ratio was significantly improved as the barium sulfate deposition was prevented. Among the examined inhibitors, the least formation damage occurred with the DPAAI application. The rock permeability ratios at the end of the injection process using DPAAI, DTPMP, PBTC, and HMDP were 0.946, 0.879, 0.859, and 0.809, respectively. As explained in Sect. 3.3., the high inhibition performance of DPAAI in preventing barium sulfate precipitation is associated with the adsorption of its components on salt crystals and a decrease in the growth rate. In all experiments, among the well-known industrial reagents, DTPMP had the highest inhibition performance for controlling barium sulfate precipitation. The inhibition mechanism is associated with the strong interaction between the molecules of the studied inhibitors and the surface of barite crystals, which reduces the growth of crystals. In this case, the surface of the formed crystals is covered with the adsorbed inhibitor molecules [51]. The interaction and coverage of barite crystals in the presence

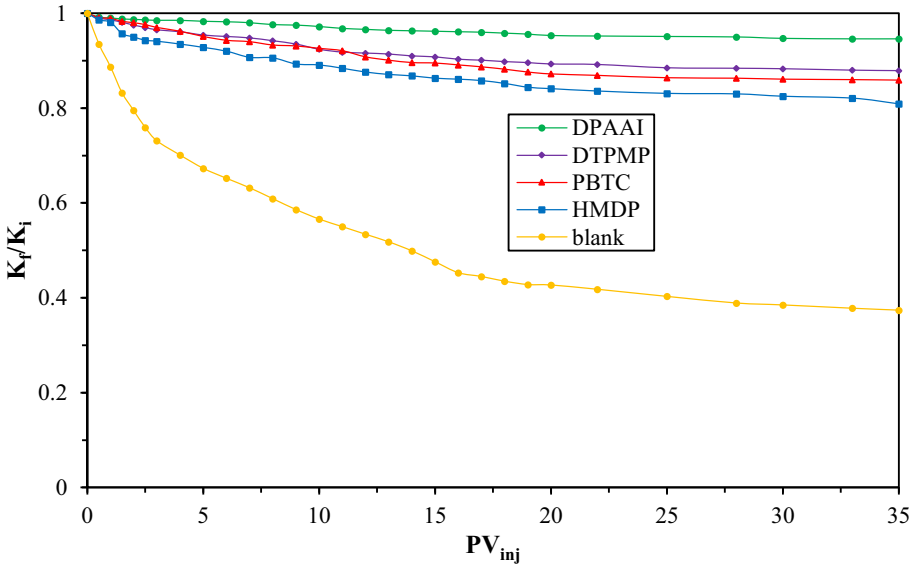

Fig. 7 Changes in the rock permeability due to the salt precipitation at a constant injection rate of 3 mL/min

of DPAAI were stronger than industrial scale inhibitors. Furthermore, the SEM images (Scanning Electron Microscopy) of barite particles in the presence of studied scale inhibitors including DPAAI (new package) can be useful to better understand the inhibition mechanism of the reagents. Therefore, it is a topic for future work to determine crystallization kinetics, surface coverage, and the size and morphology of the crystals in the presence of inhibitors.

In addition, the effect of injection rate on the permeability reduction ratio (K_f/K_i) was evaluated in coreflood tests without the use of scale inhibitors. The tests were completed at injection rates of 2, 3, and 4 mL/min. The obtained results are shown in Table 8. As can be seen from this table, the permeability reduction due to barite precipitation was decreased by increasing the injection rate. As mentioned above in coil tube tests, this is due to a reduction in the contact time of the waters during the tests, resulting in a reduced possibility of combing barium and sulfate ions. Similar results on the effect of injection rate on permeability reduction due to barite precipitation were reported by Manzari Tavakoli et al. [16]. In addition, the pressure drop and permeability reduction ratio in coreflood tests were evaluated in the presence of DPAAI at injection rates of 2, 3, and 4 mL/min. In this case, the mixture was used at 20 ppm. The results showed the rock permeability in the presence of this package was not significantly affected by the injection rate, and formation damage was not high at all injection rates. The results were similar to those shown for DPAAI in Fig. 7 at all three injection rates.

K_f/K_i ratios obtained from the coreflood tests in the blank case were used to develop a novel model for predicting permeability changes owing to $BaSO_4$ salt. In this case, the experiments were carried out at various values of temperature, injection rate, and pore volume injected. The obtained experimental values of permeability ratio were compared

Table 8 The effect of injection rate on the permeability reduction ratio (K_f/K_i) in the absence of scale inhibitors

PV_{inj}	Permeability reduction ratio (K_f/K_i) without the use of inhibitors		
	2 mL/min	3 mL/min	4 mL/min
0.0	1.000	1.000	1.000
0.5	0.907	0.935	0.953
1.0	0.853	0.887	0.919
1.5	0.792	0.832	0.865
2.0	0.768	0.795	0.822
2.5	0.719	0.759	0.784
3.0	0.667	0.731	0.763
4.0	0.627	0.701	0.727
5.0	0.596	0.673	0.691
7.0	0.564	0.632	0.659
10.0	0.503	0.566	0.590
12.0	0.477	0.534	0.564
15.0	0.409	0.476	0.501

with the predicted values using various models. Among the used models, the following models had the best agreement between the experimental and predicted values of permeability ratio: Tahmasebi et al. [53]; Hajirezaie et al. [54]; Khormali et al. [55].

Tahmasebi et al. [53] used a novel formula to forecast damaged permeability because of $CaSO_4$ in the porous media. They emphasized that in the study of permeability reduction due to scaling, it is necessary to systematically take into account a set of important parameters affecting this complex process. Their model is presented as follows:

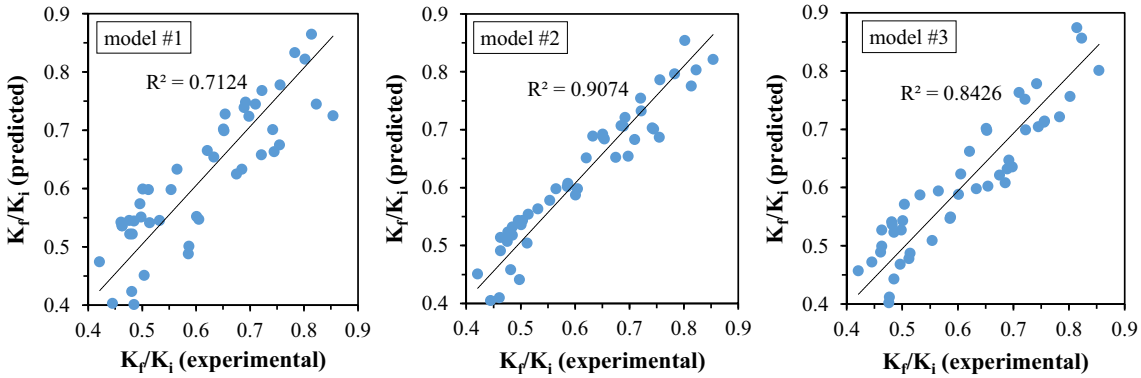

Fig. 8 The comparison of experimental and predicted data of rock permeability changes due to $BaSO_4$ using three different models

Model #1:

$$\frac{K_f}{K_i} = \exp\left(-PV_{inj}\frac{\varphi A\left(\frac{T}{40}\right)^{0.5}(SS-1)^{1.5}}{HM \times SP \times q}\right) \tag{7}$$

where K_f and K_i are final and initial values of the rock permeability (mD); PV_{inj} is pore volume injected (unitless); ϕ is the porosity of the rock samples (unitless); A is the cross-sectional area of the rock samples (cm^2); T is the temperature (°C); SS is supersaturation index of anhydrite (unitless); HM is a function of supersaturation index and volume rate (unitless); SP (surface property) is a coefficient; q is the injection rate (mL/min).

Hajirezaie et al. [54] suggested a new formula in order to predict the changes in the damaged permeability owing to barium sulfate precipitation at various concentrations. The model was based on a multivariate regression analysis. The model is expressed as follows:

Model #2:

$$\begin{aligned}\exp\left(\frac{K_f}{K_i}\right) = {} & -1.33 + 0.789(1.8T+32)^{0.17} \\ & - 2.69\times10^{-6}(qt)^{0.25} \\ & + 6.06\ln(PV_{inj}) - 0.545\ln(C_{BS}) \\ & + 0.094\ln\left(\frac{\Delta P}{6.89}\right)\end{aligned} \tag{8}$$

where t is injection time (min); C_{BS} is barium sulfate concentration (ppm); ΔP is the pressure drop (KPa).

Khormali et al. [55] suggested a model for predicting changes in the permeability of carbonate core samples due to calcium sulfate precipitation. Their model is as follows:

Model #3:

$$\frac{K_f}{K_i} = \exp\left(-3.88PV_{inj}\frac{\varphi A\left(\frac{T}{69}\right)^{0.74}(1.4SS-1.6)^{0.95}}{q}\right) \tag{9}$$

Figure 8 shows a comparison of experimental and predicted data of rock permeability changes due to barium sulfate precipitation using the mentioned models. As presented in the figure, model #2 had the best match between experimental and predicted values of K_f/K_i. In this case, the R-squared value was 0.9074. Thus, model #2 was used as the basis to develop a more accurate model for predicting rock permeability ratio (damaged/initial) during $BaSO_4$ formation in the rock samples.

Model #2 was used in order to obtain a modified correlation with high accuracy in the prediction of rock permeability ratio. The correlation was developed using the experimental values of permeability ratio (K_f/K_i) without the use of reagents (a blank case) in the MATLAB program. The development of the model was completed by changing the coefficients and powers of parameters in model #2. For this purpose, the predicted data were compared with experimental data by minimizing the sum of squared errors. The new model is as follows:

$$\begin{aligned}\exp\left(\frac{K_f}{K_i}\right) = {} & -2.07 + 2.174(1.8T+32)^{0.28} \\ & - 7.15\times10^{-3}(q)^{0.42}(t)^{0.33} \\ & + 3.01\ln(PV_{inj}) - 1.247\ln(C_{BS}) \\ & + 0.845\ln\left(\frac{\Delta P}{6.89}\right)\end{aligned} \tag{10}$$

To evaluate the accuracy of the developed model, the R^2-statistics were used in this work. In this case, R^2 (coefficient of determination), adjusted-R^2, and predicted-R^2 were utilized to determine how the proposed model fits the experimental data. In this case, the R^2 value between the data was 0.9877, indicating a high significance of the developed model. Moreover, the predicted-R^2 value (0.9868) reasonably agrees with the adjusted-R^2 (0.9875) since their difference is less than 0.2 [56], which indicates the high

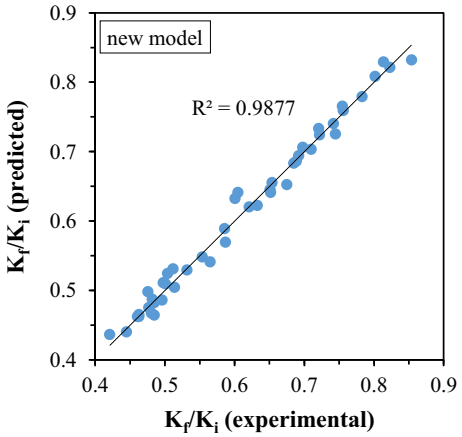

Fig. 9 The comparison of experimental and predicted data of rock permeability changes due to $BaSO_4$ using the new model

precision of the new model in predicting formation damage owing to BaSO4. Besides, the comparison of predicted data of permeability ratio with the experimental data is illustrated in Fig. 9. As shown in the figure, the data predicted by the model were in good agreement with the experimental results. Therefore, the developed model (Eq. 10) can be used for the prediction of rock permeability in the reservoirs, where barium sulfate is precipitated. It should be noted that to develop this model, various core flood tests under different values of the parameters (injection rate, temperature, time, pressure drop, and barium sulfate concentration) have been conducted. As mentioned above, the model was developed using the experimental data through MATLAB, which is useful for predicting formation damage under barite deposition conditions. By knowing the amount of permeability reduction, it is possible to control the scaling process in time and use the required concentration of the inhibitors for effective inhibition. Moreover, to evaluate the effect of injection rate, temperature, time, pressure drop, and barium sulfate concentration on the permeability reduction ratio, the analysis of variance (ANOVA) can be applied as a useful tool to determine the significance of the parameters as well as the developed model. This can be accomplished by plotting one factor, contour, and 3-D surface graphs. Therefore, it will be a topic for our future work.

3.7 Experimental and Modeling Analysis of the Scale Inhibitor Return Concentration

Coreflood experiments have been repeated to determine the inhibitor return concentration under dynamic conditions. In this case, MIC obtained in the coil tests was used as the effective concentration of the scale inhibitors. At first, the inhibitor adsorption was completed on the rock surface. Then, the desorption process was investigated to determine the protection period of the near-wellbore region from the barium sulfate precipitation by analyzing the scale inhibitor return concentration. It should be noted that long-term protection of wells and near-wellbore region from scale precipitation occurs in a slow desorption process [23, 31]. Figure 10 depicts the dependence of the concentration ratio (C_f/C_i) of scale inhibitors PV_{inj}. Here, C_f and C_i represent the final and initial concentrations of scale inhibitors (at outlet and inlet). As presented in Fig. 10, at the beginning of the desorption process, C_f/C_i dropped sharply to almost 5 PV_{inj}. A concentration ratio of 0.005 was considered the minimum required value for the control of barium sulfate precipitation. Among the studied scale inhibitors, DPAAI had the longest desorption process. It should be noted that the desorption behavior of the studied inhibitors is associated with the fact their molecules act as adsorbates to the crystals of barium sulfate particles and reduce the crystal growth rate [57]. Therefore, the inhibition process in the presence of the used inhibitors can be described by the adsorption of their molecules to the crystals of barium sulfate particles. MIC values of DPAAI, DTPMP, PBTC, and HMDP were observed after 32, 28, 25, and 22 PV_{inj}. Thus, the protection period with DPAAI is longer than the industrial reagents. Specifically, it is related to the high performance of the DPAAI in preventing salt precipitation and its good compatibility with the reservoir rock. This ability was provided by the active components of DPAAI. Also, the reaction between particles of barium sulfate and the inhibitor molecules in the presence of DPAAI is more entropy favored than studied industrial reagents [57, 58].

The obtained curves of the scale inhibitor return concentration (Fig. 10) were processed using the Squeeze program to determine the protection period of the well and near-wellbore region from the barium sulfate precipitation. The input data for the modeling were the concentration ratio of scale inhibitors at various values of pore volume injected. In addition, the Freundlich isotherm was utilized to complete the modeling. In this case, k and n (constants of the Freundlich isotherm) were 35 and 0.52, respectively. Moreover, the initial porosity and permeability were 0.18 and 27 mD. The modeling has been performed with the following volumes of the reagents: 4 and 8 m^3. Figure 11 illustrates simulation results of the return scale inhibitor concentration over 300 days of production. As shown in the figure, the longest squeeze lifetime was achieved by DPAAI in both cases (4 and 8 m^3). Among the industrial reagents, DTPMP had the longest return profile of concentration. The protection periods of the near-wellbore region and well with an injection volume of 4 m^3 using DPAAI, DTPMP, PBTC, and HMDP were 152, 116, 98, and 72 days, respectively. In addition, with an injection volume of 8 m^3 of DPAAI, DTPMP, PBTC, and HMDP, the protection period was about 163, 130, 109, and 82 days, respectively. Therefore, with an increase in the

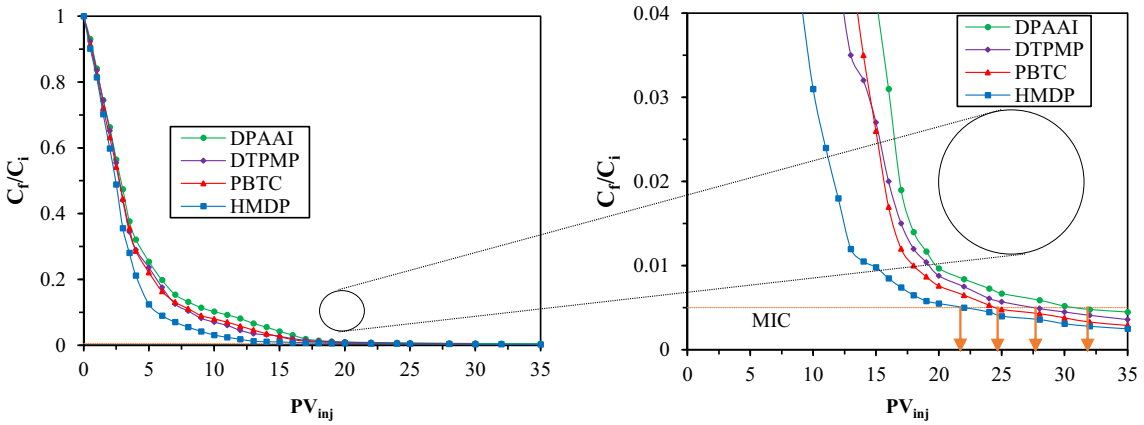

Fig. 10 Experimental analysis of the scale inhibitor return concentration

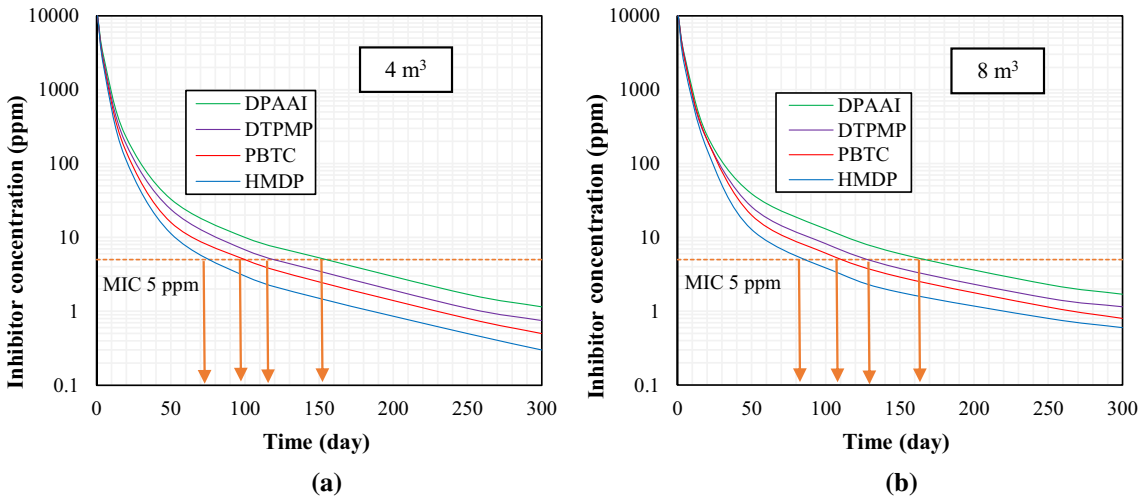

Fig. 11 Modeling analysis of the return scale inhibitor concentration with 4 m^3 **a**, and 8 m^3 **b**

injection volume from 4 to 8 m^3, the protection time from scaling was increased by about 10%.

Finally, the techno-economic analysis of the process of injecting the developed mixture of reagents (DPAAI) into oil wells was carried out in order to inhibit the formation of barium sulfate. The analysis was performed by comparing the estimated cost of the application of the developed mixture of reagents with the average cost of the studied industrial scale inhibitors (DTPMP, PBTC, ATMP, and HMDP) and determining the cost reduction due to a decrease in the mean time to repair the production equipment. The results of the analysis showed that the use of the developed mixture of reagents makes it possible to reduce the operating costs in the production well by about 9% compared to the indicated industrial scale inhibitors. It is associated with the high performance of the proposed mixture for barite control, as well as its longer protection period of the equipment, which allows to increase the mean time to repair the production equipment. The results of the techno-economic analysis may vary from country to country due to differences in operating costs and field conditions.

The proposed mixture (DPAAI) has good potential for field application due to excellent results in various laboratory tests compared to industrial scale inhibitors and lower cost of operation. Thus, the mixture will be used in the future for the inhibition of barite in real conditions of oil reservoirs. Moreover, DPAAI has already been applied in the real field for the prevention of simultaneous formation of calcium and strontium sulfate scales, the results of which were presented in our previous work [8].

4 Summary and Conclusions

1. Scaling tendency, saturation index and concentration of $BaSO_4$ salt were predicted over a wide range of mixing ratios of formation and injection waters under ambient and reservoir conditions. The worst scenario of barium sulfate

precipitation occurred at a ratio of 40:60 FW:IW. The amount of barium sulfate precipitation under reservoir conditions was less than under ambient conditions due to an increase in the salt solubility by increasing the pressure and temperature.

2. A critical radius and mass of barium sulfate particles were determined, depending on the supersaturation ratio in the absence of scale inhibitors. At surface tensions of 58 and 113 mN/m, the critical supersaturation ratio with $BaSO_4$ was 3 and 4. The solubility of barium sulfate was significantly decreased when the concentration and supersaturation ratio exceeded the critical value.

3. The results of jar test (in static conditions) demonstrated that the optimal concentration of inhibitors was about 20 ppm (for DPAAI, DTPMP) and 25 ppm (for PBTC, HMDP). The inhibition performance of DPAAI, DTPMP, PBTC, and HMPD at the optimal concentrations was 95.7, 88.5, 87.5, and 85.9%, respectively. DPAAI as a multicomponent scale inhibitor showed a positive synergistic inhibition effect that prevented the heterogeneous nucleation of barium sulfate. In addition, the chances of collisions between cations and anions in the solution were reduced in the presence of DPAAI. Moreover, DPAAI could specifically adsorb the crystals of barium sulfate, slow down the crystal growth rate, and keep them in the solution in suspension. Meantime, an increase in the concentration of barium ions did not have a significant effect on the prevention efficiency of the studied reagents.

4. Turbidly tests depicted that the performance of $BaSO_4$ inhibition was increased with an increase in the concentration of the reagents. It was related to the suspended state of the solid particles and a reduction in the light intensity passing through the working solution. Furthermore, after the addition of HMDP, PBTC, DTPMP, and DPAAI to the solution, the critical supersaturation ratios with barium sulfate salts were 4000, 5000, 6000, and 7000, respectively, which are rather high values. MIC values of the scale inhibitors for dynamic conditions were analyzed by conducting dynamic tube blocking tests. MIC values of DPAAI, DTPMP, PBTC, and HMPD were 20, 20, 25, and 25 ppm, respectively. At the obtained concentrations, the precipitation of barium sulfate did not occur owing to its complete prevention.

5. The decrease in rock permeability because of $BaSO_4$ precipitation was investigated with and without the addition of reagents to the solution. In a blank case, the permeability ratio (damaged/initial) was less than 0.4 at the end of the injection process. In addition, the rock permeability ratio at the end of the injection process using DPAAI, DTPMP, PBTC, and HMDP was 0.946, 0.879, 0.859, and 0.809. Accordingly, DPAAI demonstrated the best performance for controlling the formation of $BaSO_4$ in the rock samples. The high inhibition performance of DPAAI in preventing barium sulfate precipitation was associated with the adsorption of its components on the crystals and a decrease in the growth rate. Moreover, a new model has been proposed for predicting formation damage by $BaSO_4$ precipitation. The model had high accuracy, in which the R-squared value between experimental and predicted data of rock permeability was 0.9877.

6. Modeling of the process of squeezing the scale inhibitor into the reservoir, determination of protection period from the salt precipitation, and optimization of the injected volumes was carried out using the Squeeze program. The main result of the simulation was the evaluation of scale inhibitor return concentration and the basic design of the injection technology. The simulation results indicated that the effective inhibition period (squeeze lifetime) of the near-wellbore region and equipment from barium sulfate precipitation with an injection volume of 4 m^3 using DPAAI, DTPMP, PBTC, and HMDP was 152, 116, 98, and 72 days, respectively.

7. An economic analysis for the DPAAI injection process into the oil wells was performed. The analysis was completed by comparing the estimated cost of the application of DPAAI with the cost of the commercial scale inhibitors. In the case of inhibiting scale in the wells, the cost of one treatment using DPAAI and the industrial inhibitors approximately was the same. In addition, the inhibition efficiency and protection period with the use of DPAAI was better than the industrial inhibitors.

Acknowledgements This work was funded and supported by Iran's National Elites Foundation (INEF) based on Dr. Kazemi Ashtiani Research Grant Award for Young Assistant Professors (to Dr. Azizollah Khormali).

References

1. Luo, H.; Chen, D.; Yang, X.; Zhao, X.; Feng, H.; Li, M.; Wang, J.: Synthesis and performance of a polymeric scale inhibitor for oilfield application. J. Petrol. Explor. Product. Technol. **5**, 177–187 (2015). https://doi.org/10.1007/s13202-014-0123-0
2. Li, J.; Tang, M.; Ye, Z.; Chen, L.; Zhou, Y.: Scale formation and control in oil and gas fields: a review. J. Dispers. Sci. Technol. **38**(5), 661–670 (2017). https://doi.org/10.1080/01932691.2016.1185953
3. Kamal, M.S.; Hussein, I.; Mahmoud, M.; Sultan, A.S.; Saadd, M.A.S.: Oilfield scale formation and chemical removal: a review. J. Petrol. Sci. Eng. **171**, 127–139 (2018). https://doi.org/10.1016/j.petrol.2018.07.037
4. Sanni, O.S.; Bukuaghangin, O.; Charpentier, T.V.; Neville, A.: Evaluation of laboratory techniques for assessing scale inhibition efficiency. J. Petrol. Sci. Eng. **182**, 106347 (2019). https://doi.org/10.1016/j.petrol.2019.106347
5. Qazvini, S.; Golkari, A.; Azdarpour, A.; Santos, R.M.; Safavi, M.S.; Norouzpour, M.: Experimental and modelling approach to investigate the mechanisms of formation damage due to calcium carbonate precipitation in carbonate reservoirs. J. Petrol. Sci. Eng. **205**, 108801 (2021). https://doi.org/10.1016/j.petrol.2021.108801
6. Kelland, M.A.: Effect of various cations on the formation of calcium carbonate and barium sulfate scale with and without scale inhibitors. Ind. Eng. Chem. Res. **50**(9), 5852–5861 (2011). https://doi.org/10.1021/ie2003494

7. Zuo, Z.; Yang, W.; Zhang, K.; Chen, Y.; Li, M.; Zuo, Y.; Yin, X.; Liu, Y.: Effect of scale inhibitors on the structure and morphology of $CaCO_3$ crystal electrochemically deposited on TA1 alloy. J. Colloid Interface Sci. **562**, 558–566 (2020). https://doi.org/10.1016/j.jcis.2019.11.078
8. Khormali, A.; Bahlakeh, G.; Struchkov, I.; Kazemzadeh, Y.: Increasing inhibition performance of simultaneous precipitation of calcium and strontium sulfate scales using a new inhibitor—Laboratory and field application. J. Petrol. Sci. Eng. **202**, 108589 (2021). https://doi.org/10.1016/j.petrol.2021.108589
9. Spinthaki, A.; Kamaratou, M.; Skordalou, G.; Petratos, G.; Tramaux, A.; David, G.; Demadis, K.D.: A universal scale inhibitor: a dual inhibition/dispersion performance evaluation under difficult brine stresses. Geothermics **89**, 101972 (2021). https://doi.org/10.1016/j.geothermics.2020.101972
10. BinMerdhah, A.B.: Inhibition of barium sulfate scale at high-barium formation water. J. Petrol. Sci. Eng. **90–91**, 124–130 (2012). https://doi.org/10.1016/j.petrol.2012.04.005
11. Collins, IR; (2005) Predicting the location of barium sulfate scale formation in production systems. Presented at the SPE International Symposium on Oilfield Scale, Aberdeen, United Kingdom, Article number SPE-94366-MS. https://doi.org/10.2118/94366-MS.
12. Khormali, A.; Petrakov, DG.; Lamidi, ALB.; Rastegar, R.; Prevention of calcium carbonate precipitation during water injection into high-pressure high-temperature wells. presented at the SPE European Formation Damage Conference and Exhibition, Budapest, Hungary, Article number SPE-174277-MS. (2015) https://doi.org/10.2118/174277-MS.
13. Ruiz-Agudo, C.; Ruiz-Agudo, E.; Putnis, C.V.; Putnis, A.: Mechanistic principles of barite formation: from nanoparticles to micron-sized crystals. Cryst. Growth Des. **15**(8), 3724–3733 (2015). https://doi.org/10.1021/acs.cgd.5b00315
14. Ronquim, F.M.; Cotrim, M.E.B.; Guilhen, S.N.; Bernardo, A.; Seckler, M.M.: Improved barium removal and supersaturation depletion in wastewater by precipitation with excess sulfate. J. Water Process Eng. **23**, 265–276 (2018). https://doi.org/10.1016/j.jwpe.2018.04.007
15. Mavredaki, E.; Neville, A.; Sorbie, K.S.: Initial stages of barium sulfate formation at surfaces in the presence of inhibitors. Cryst. Growth Des. **11**(11), 4751–4758 (2011). https://doi.org/10.1021/cg101584f
16. Manzari Tavakoli, H.; Jamialahmadi, M.; Kord, S.; Daryasafar, A.: Experimental investigation of the effect of silica nanoparticles on the kinetics of barium sulfate scaling during water injection process. J. Petrol. Sci. Eng. **169**, 344–352 (2018). https://doi.org/10.1016/j.petrol.2018.05.077
17. Akyol, E.; Cedimagar, M.A.: Size and morphology controlled synthesis of barium sulfate. Cryst. Res. Technol. **51**(6), 393–399 (2016). https://doi.org/10.1002/crat.201600046
18. Abd-El-Khalek, D.E.; Abd-El-Nabey, B.A.; Abdel-kawi, M.A.; Ebrahim, S.; Ramadan, S.R.: The inhibition of crystal growth of gypsum and barite scales in industrial water systems using green antiscalant. Water Supply **19**(7), 2140–2146 (2019). https://doi.org/10.2166/ws.2019.094
19. Ko, S.; Wang, X.; Kan, A.T.; Tomson, M.B.: Growth inhibition and deposition prevention of sulfide scales using dispersants. J. Petrol. Sci. Eng. **197**, 108107 (2021). https://doi.org/10.1016/j.petrol.2020.108107
20. Athanassopoulos, E.; Rokidi, S.; Koutsoukos, PG.; Barium sulfate crystal growth and inhibition: Implications of molecular structure on scale inhibition. Presented at the CORROSION 2016, Vancouver, British Columbia, Canada, Article number (2016) NACE-2016–7460.
21. Lu, A.Y.T.; Kan, A.T.; Tomson, M.B.: Nucleation and crystallization kinetics of barium sulfate in the hydrodynamic boundary layer: an explanation of mineral deposition. Cryst. Growth Des. **21**(3), 1443–1450 (2021). https://doi.org/10.1021/acs.cgd.0c01027
22. Geng, X.; Sosa, R.D.; Reynolds, M.A.; Conrad, J.C.; Rimer, J.D.: Alginate as a green inhibitor of barite nucleation and crystal growth. Mol. Syst. Des. Eng. **6**(7), 508–519 (2021). https://doi.org/10.1039/D1ME00010A
23. He, S.; Kan, A.T.; Tomson, M.B.: Mathematical inhibitor model for barium sulfate scale control. Langmuir **12**(7), 1901–1905 (1996). https://doi.org/10.1021/la950876x
24. Carvalho, S.; Palermo, L.; Boak, L.; Sorbie, K.; Lucas, E.F.: Influence of terpolymer based on amide, carboxylic, and sulfonic groups on the barium sulfate inhibition. Energy Fuels **31**(10), 10648–10654 (2017). https://doi.org/10.1021/acs.energyfuels.7b01767
25. Wang, Y.; Li, X.; Lu, J.: Physicochemical modeling of barium and sulfate transport in porous media and its application in seawater-breakthrough monitoring. SPE J. (2021). https://doi.org/10.2118/205482-PA
26. Yuan, M.; Barium sulfate scale inhibition in the deepwater cold temperature environment. Presented at the SPE International Symposium on Oilfield Scale, Aberdeen, United Kingdom, Article number SPE-68311-MS. (2001) https://doi.org/10.2118/68311-MS.
27. Shaw, S.S.; Sorbie, K.S.: Synergistic properties of phosphonate and polymeric scale-inhibitor blends for barium sulfate scale inhibition. SPE Product. Oper. **30**(1), 16–25 (2014). https://doi.org/10.2118/169752-PA
28. Chew, C.; Mat, R.: The efficacy of calcium carbonate scale inhibition by commercial polymer scale inhibitors. Chem. Eng. Trans. **45**, 1471–1476 (2015). https://doi.org/10.3303/CET1545246
29. Chao, J.; Zhang, L.; Feng, T.; Wang, Z.; Xu, S.; Zhang, C.; Ren, S.: Experimental study on the compatibility of scale inhibitors with mono ethylene glycol. Petrol. Res. **5**(4), 315–325 (2020). https://doi.org/10.1016/j.ptlrs.2020.07.003
30. Ishtiaq, U.; Muhsan, A.S.; Rozali, A.S.; Mohamed, N.M.; Badri Albarody, T.M.: Graphene oxide/carbon nanotubes nanocoating for improved scale inhibitor adsorption ability onto rock formation. J. Petrol. Explor. Product. Technol. **10**, 149–157 (2020). https://doi.org/10.1007/s13202-019-0689-7
31. Jarrahian, K.; Sorbie, K.; Singleton, M.; Boak, L.; Graham, A.: Building a fundamental understanding of scale-inhibitor retention in carbonate formations. SPE Prod. Oper. **35**(1), 85–97 (2020). https://doi.org/10.2118/193635-PA
32. Stamatiou, A.; Sorbie, K.S.: Analytical solutions for a 1D scale inhibitor transport model with coupled adsorption and precipitation. Transp. Porous Media **132**(3), 591–625 (2020). https://doi.org/10.1007/s11242-020-01405-0
33. Zhang, P.; Ruan, G.; Shen, D.; Kan, A.T.; Tomson, M.: Transport and return of an oilfield scale inhibitor reverse micelle nanofluid: Impact of preflush and overflush. RSC Adv. **6**(71), 66672–66681 (2016). https://doi.org/10.1039/C6RA07445F
34. Al-Sabagh, A.M.; Basiony, N.M.E.; Sadeek, S.A.; Migahed, M.A.: Scale and corrosion inhibition performance of the newly synthesized anionic surfactant in desalination plants: experimental, and theoretical investigations. Desalination **437**, 45–48 (2018). https://doi.org/10.1016/j.desal.2018.01.036
35. Moghadasi, R.; Rostami, A.; Tatar, A.; Hemmati-Sarapardeh, A.: An experimental study of Nanosilica application in reducing calcium sulfate scale at high temperatures during high and low salinity water injection. J. Petrol. Sci. Eng. **179**, 7–18 (2019). https://doi.org/10.1016/j.petrol.2019.04.021
36. Jarrahian, K.; Singleton, M.; Boak, L.; Sorbie, K.S.: Surface chemistry of phosphonate scale inhibitor retention mechanisms in carbonate reservoirs. Cryst. Growth Des. **20**(8), 5356–5372 (2020). https://doi.org/10.1021/acs.cgd.0c00570

37. Zhang, P.: Review of synthesis and evaluation of inhibitor nanomaterials for oilfield mineral scale control. Front. Chem. **8**, 576055 (2020). https://doi.org/10.3389/fchem.2020.576055
38. Wang, Y.; Li, A.; Yang, H.: Effects of substitution degree and molecular weight of carboxymethyl starch on its scale inhibition. Desalination **408**, 60–69 (2017). https://doi.org/10.1016/j.desal.2017.01.006
39. Jafar Mazumder, M.A.: A Review of green scale inhibitors: process, types, mechanism and properties. Coatings **10**(10), 1–29 (2020). https://doi.org/10.3390/coatings10100928
40. Karar, A.; Henni, A.: Scale inhibition in hard water system. water resources in Algeria - part I. Handb. Environ. Chem. **97**, 293–318 (2020). https://doi.org/10.1007/698_2020_530
41. Rabizadeh, T.; Peacock, C.L.; Benning, L.G.: Investigating the effectiveness of phosphonate additives in hindering the calcium sulfate dihydrate scale formation. Ind. Eng. Chem. Res. **59**(33), 14970–14980 (2020). https://doi.org/10.1021/acs.iecr.0c03600
42. Gamal, H.; Elkatatny, S.; Al-Afnan, S.; Bahgat, M.: Development of a unique organic acid solution for removing composite field scales. ACS Omega **6**(2), 1205–1215 (2021). https://doi.org/10.1021/acsomega.0c04335
43. Zhu, Y.; Li, H.; Zhu, M.; Wang, H.; Li, Z.: Dynamic and active antiscaling via scale inhibitor pre-stored superhydrophobic coating. Chem. Eng. J. **403**, 126467 (2021). https://doi.org/10.1016/j.cej.2020.126467
44. Mady, M.F.; Bayat, P.; Kelland, M.A.: Environmentally friendly phosphonated polyetheramine scale inhibitors - excellent calcium compatibility for oilfield applications. Ind. Eng. Chem. Res. **59**(21), 9808–9818 (2020). https://doi.org/10.1021/acs.iecr.0c01636
45. Kommanapalli, K.K.; Lyot, P.; Sunkara, J.R.; Cheucle, P.; Hari Haran, A.V.L.N.S.H.; Mulukutla, P.: Synthesis and characterization of maleic acid and sodium methallyl disulfonate new copolymer: application as a barium sulfate scale inhibitor. J. Petrol. Explor. Product. Technol. **9**(1), 223–232 (2019). https://doi.org/10.1007/s13202-018-0450-7
46. Khormali, A.; Petrakov, D.G.; Nazari Moghaddam, R.: Study of adsorption/ desorption properties of a new scale inhibitor package to prevent calcium carbonate formation during water injection in oil reservoirs. J. Petrol. Sci. Eng. **153**, 257–267 (2017). https://doi.org/10.1016/j.petrol.2017.04.008
47. Macedo, R.G.; Marques, N.D.; Paulucci, L.C.S.; Cunha, J.V.M.; Villetti, M.A.; Castro, B.B.; Balaban, R.D.: Water-soluble carboxymethylchitosan as green scale inhibitor in oil wells. Carbohyd. Polym. **215**, 137–142 (2019). https://doi.org/10.1016/j.carbpol.2019.03.082
48. Khormali, A.; Petrakov, D.G.; Moein, M.J.A.: Experimental analysis of calcium carbonate scale formation and inhibition in waterflooding of carbonate reservoirs. J. Petrol. Sci. Eng. **147**, 843–850 (2016). https://doi.org/10.1016/j.petrol.2016.09.048
49. Steiger, M.: Crystal growth in porous materials—I: the crystallization pressure of large crystals. J. Cryst. Growth **282**(3–4), 455–469 (2005). https://doi.org/10.1016/j.jcrysgro.2005.05.007
50. Jiang, S.H.; Joop, H.: Crystal nucleation rates from probability distributions of induction times. Cryst. Growth Des. **11**(1), 256–261 (2011). https://doi.org/10.1021/cg101213q
51. Wang, F.; Xu, G.; Zhang, Z.; Song, S.; Dong, S.: A systematic morphosynthesis of barium sulfate in the presence of phosphonate inhibitor. J. Colloid Interface Sci. **293**(2), 394–400 (2006). https://doi.org/10.1016/j.jcis.2005.06.060
52. Moghadasi, J.; Jamialahmadi, M.; Müller-Steinhagen, H.; Sharif, A.: Scale formation in oil reservoir and production equipment during water injection (kinetics of $CaSO_4$ and $CaCO_3$ crystal growth and effect on formation damage). Presented at the SPE European Formation Damage Conference, The Hague, Netherlands, Article number SPE-82233-MS (2003). https://doi.org/10.2118/82233-MS
53. Tahmasebi, H.A.; Kharrat, R.; Soltanieh, M.: Dimensionless correlation for the prediction of permeability reduction rate due to calcium sulphate scale deposition in carbonate grain packed column. J. Taiwan Inst. Chem. Eng. **41**(3), 268–278 (2010). https://doi.org/10.1016/j.jtice.2009.11.006
54. Hajirezaie, S.; Wu, X.; Peters, C.A.: Scale formation in porous media and its impact on reservoir performance during water flooding. J. Nat. Gas Sci. Eng. **39**, 188–202 (2017). https://doi.org/10.1016/j.jngse.2017.01.019
55. Khormali, A.; Sharifov, A.R.; Torba, D.I.: Increasing efficiency of calcium sulfate scale prevention using a new mixture of phosphonate scale inhibitors during waterflooding. J. Petrol. Sci. Eng. **164**, 145–258 (2018). https://doi.org/10.1016/j.petrol.2018.01.055
56. Ahmadi, S.; Khormali, A.; Khoutoriansky, F.M.: Optimization of the demulsification of water-in-heavy crude oil emulsions using response surface methodology. Fuel **323**, 124270 (2022). https://doi.org/10.1016/j.fuel.2022.124270
57. Lu, A.Y.T.; Shi, W.; Wang, J.; Venkatesan, R.; Harouaka, K.; Paudyal, S.; Ko, S.; Dai, C.; Gao, S.; Deng, G.; Zhao, Y.; Wang, X.; Kan, A.T.; Tomson, M.: The mechanism of barium sulfate deposition inhibition and the prediction of inhibitor dosage. J. Chem. Eng. Data **64**(11), 4968–4976 (2019). https://doi.org/10.1021/acs.jced.9b00799
58. Adamson, A.W.: Physical chemistry of surfaces. Wiley, New York (1990)